PHYSICAL REVIEW E **81**, 045201(R) (2010)

Fast reciprocal inhibition can synchronize bursting neurons

Sajiya Jalil, Igor Belykh, and Andrey Shilnikov
Department of Mathematics and Statistics and Neuroscience Institute, Georgia State University, 30 Pryor Street, Atlanta, Georgia 30303, USA

(Received 10 July 2009; revised manuscript received 13 March 2010; published 23 April 2010)

We study a pair of endogenously bursting neurons with fast nondelayed inhibitory connections. We show that fast reciprocal inhibition, known to facilitate antiphase bursting, can stably synchronize bursting neurons. This contrasts with the classical view that reciprocal inhibition has to be slow or time delayed to establish in-phase synchronization. Through stability analysis, we reveal the emergent mechanism of in-phase synchronization and discuss its implications for various types of bursting neurons and networks.

DOI: 10.1103/PhysRevE.81.045201 PACS number(s): 05.45.Xt, 87.19.L−

Reciprocal inhibition is the key component for functioning of various regulatory and neural networks such as central pattern generators (CPGs) [1–3]. CPGs are small polymorphic neural circuits governing various rhythmic activities including cardiac beating and locomotive behaviors such as walking, chewing, and swimming [3]. Switching between locomotion behaviors can be attributed to switching between various attractors of a CPG network. Each attractor is associated with a definite rhythm on a specific time scale. Such a multifunctional CPG contrasts to a dedicated CPG that is only capable of generating a single robust rhythm [3]. A building block of many CPGs is a half-center oscillator [1], composed of two cells reciprocally inhibiting each other to produce alternating dynamics in which each cell engages in antiphase bursting. There has been much work on the mechanisms giving rise to antiphase bursting, including the synaptic release, the postinhibitory rebound, and the synaptic escape [2,4]. The network circuitry and the synaptic and intrinsic properties of cells cooperate synergetically to produce a plethora of cooperative rhythms [4–19].

Reciprocal inhibition is postulated to desynchronize neurons, provided that inhibition is fast [4,7,10,11]; i.e., the synaptic decay is faster than or comparable to the duration of presynaptic drive. More precisely, it was shown that stable synchronous oscillations are not possible in reciprocally coupled networks of fast inhibitory *spiking* cells [10,11], unless each spiking cell has at least two slow intrinsic variables [9]. At the same time, a slowly decaying inhibition or a time delay does establish synchronization in the network [2,4,7,10,11]. In particular, it was demonstrated [7] that inhibition, not excitation, leads to synchronized firing, provided that reciprocal synapses are noninstantaneous and slow. Furthermore, such a network can exhibit coexistent in-phase and antiphase synchronized firing [4,7].

In this Rapid Communication, we report that *fast* nondelayed reciprocal inhibition can synchronize endogenously *bursting* cells. We reveal the mechanisms of in-phase synchronization, which are specifically due to the spike interactions of the cells during the active phase of bursting. This contrasts to the solely desynchronizing properties of relaxation oscillators which are often used to model bursting cells where the spikes are omitted [2,11]. In our case the stable in-phase synchronization coexists with antiphase bursting within a broad range of initial conditions and parameter values of the network. We provide a quantitative analysis of the stability conditions through the examination of the variational equation and reveal the properties of the network model that make in-phase synchronization stable. Our finding and tools are applicable to a variety of oscillatory cells [14], as well as to large complex networks in general.

The two-cell network of endogenously bursting cells in the study is described within the framework of the Hodgkin-Huxley formalism

$$CV_i' = F(V_i,h_i,m_i) - g_s(V_i - E_s)\Gamma(V_j - \Theta_{syn}),$$

$$\tau_h h_i' = G(V_i,h_i), \quad \tau_m m_i' = R(V_i,m_i), \quad i,j = 1,2, \qquad (1)$$

where V_i, h_i, and m_i are the ith neuron nondimensionalized membrane potential and the gating variables for the fast sodium and the slow potassium currents in a reduced model of the leech heart CPG interneuron [6]. The inhibitory synapses are instantaneous and described through the fast threshold modulation (FTM) concept [12], where the coupling function is given by $\Gamma(V_j-\Theta_{syn})=1/[1+\exp\{-1000(V_j-\Theta_{syn})\}]$. The synaptic threshold Θ_{syn} is set to ensure that spikes within a burst cross it through, such as in Fig. 1(a). The FTM coupling is a remarkably good model of realistic fast synapses [2,11]. For instance, the rise time of the synapse in the leach heart CPG is comparable with the duration of a spike, and the synapse is nearly instantaneous [15]. The low level of reversal potential $E_s=-0.0625$ makes the synapse inhibitory. We employ the level of Θ_{syn} and the coupling strength g_s as two bifurcation parameters of network (1). Network (1) was shown to generate robust antiphase bursting via the hold-and-release mechanism [19], similar to synaptic release [2,4] in spiking cells. Observe that network (1) of two identical cells always possesses a symmetric solution $\{V:V_1(t)=V_2(t), h:h_1(t)=h_2(t), m:m_1(t)=m_2(t)\}$, corresponding to completely synchronous bursting and governed by the self-connected system known as autapse. This synchronous solution is unstable in the absence of coupling. In what follows, we will show that this synchronous bursting solution is stable and robust under quite general conditions on the inhibitory coupling. This makes the network *bistable* such that antiphase bursting and synchronous in-phase bursting coexist for the same parameter values (see Fig. 1). We also reveal the robustness of in-phase bursting with respect to transversal perturbations at its different phases by examining the shape of the attraction basin along the orbit. Figure 2 demonstrates that stable in-phase synchronization is a generic phenomenon for the two-cell network as it emerges from a wide range of

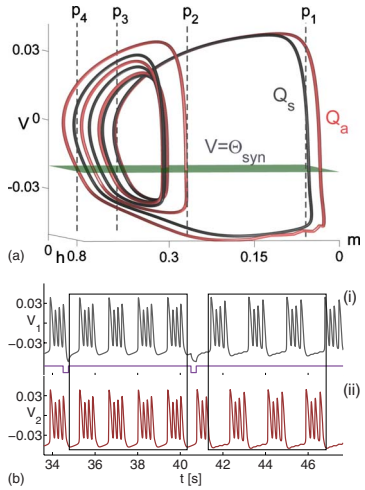

FIG. 1. (Color online) (a) Coexisting stable in-phase (Q_s) and antiphase (Q_a) bursting orbits in the phase space of Eq. (1) at $g_s=0.7$, $\Theta_{\text{syn}}=-0.02$ and $V_{\text{K2shift}}=-0.0215$. Voltage cuts p_i, $i=1,4$ reveal the V range of attraction basins (Fig. 2) of in-phase bursting at its various phases. (b). Voltage traces showing the robustness of in-phase bursting against an external pulse perturbation during the spiking period, and its vulnerability, leading to antiphase bursting, during the quiescent period of bursting.

different voltage values of both cells. This observation is reasserted by the computer-assisted verifications aimed to examine the robustness of in-phase synchronization against mismatch between the phases of the cells along the bursting orbit. Figure 3(c) shows the variations in the synchronization zone (shaded) as the cells enter the quiescent phase through tonic spiking. This is consistent with the results of Fig. 2 and confirms that in-phase synchronization is quite robust and hence achievable during the spiking phase of bursting. On

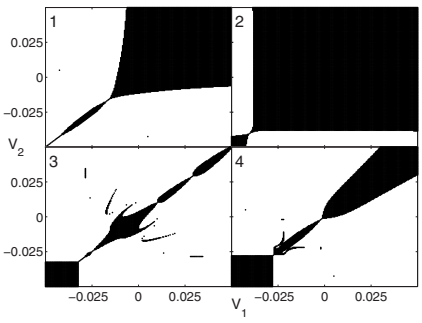

FIG. 2. Basins of attraction corresponding to the stable synchronous trajectory. The four basins of attraction (synchronization zones) in the (V_1,V_2) plane are calculated by choosing different V_1 and V_2 along the four vertical lines p_1, p_2, p_3, p_4, depicted in Fig. 1(a), that correspond to four fixed values of the gating variables $m_1=m_2$ and $h_1=h_2$. Here, $g_s=0.4$, $\Theta_{\text{syn}}=-0.0225$, and $V_{\text{K2shift}}=-0.022$. Black points indicate the initial values that converge to the synchronous trajectory (the diagonal $V_1=V_2$), whereas the white regions indicate the attraction basins of antiphase bursting. Panels 1–2 show that during the spiking phase, in-phase synchronization occurs despite a large dispersion in initial conditions in V and dominates entirely (cf. line p_2) over antiphase bursting. Panels 3–4: during the quiescence, the basins shrink strongly and become fractal.

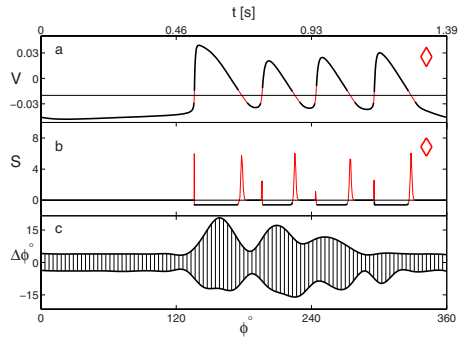

FIG. 3. (Color online) (a) Voltage trace of four-spike synchronous bursting. Its red (thin) and black (thick) segments indicate positive and negative instantaneous values of the largest transversal Lyapunov exponent $L_{\max}^{\text{inst}}$. (b) Synaptic term $S=S_1+S_2$. Note sharp positive peaks in S, corresponding to the appearance of the desynchronizing term S_2, when the bursting orbit crosses the synaptic threshold Θ_{syn}. The wide negative plateaus in S are caused by the stabilizing term S_1 and coincide with the upper part of the bursting trajectory. For the given threshold $\Theta_{\text{syn}}=-0.02$, S_1 wins over S_2 and defines the overall synchronizing effect of coupling. The corresponding averaged value of S is depicted by $\diamond$ in Fig. 4(b). (c) Shape of the synchronization basin (dashed) along bursting, parameterized from 0° through 360°; 0° corresponds to the beginning of its quiescent period. Its boundaries correspond to evolutions of unstable fixed points on the orbit which separate the basin from antiphase bursting. Tonic spiking period of bursting corresponds to the widest synchronization zone (cf. Fig. 2), while it becomes more fragile during the quiescent period: exceed of 5°, or advance of either cell's state, leads to antiphase bursting.

the other hand, a little phase mismatch between the cells during the quiescent period will likely lead to antiphase bursting. In the rest of this Rapid Communication, we explain the synchronizing effect of fast nondelayed reciprocal inhibition through examination of the variational equations for transverse perturbations to the synchronous solution [16],

$$C\xi' = F_V(V,h,m)\xi + F_h(V,h,m)\eta + F_m(V,h,m)\zeta + (S_1+S_2)\xi,$$

$$\tau_h\eta' = G_V(V,h)\xi - \eta, \quad \tau_m\zeta' = R_V(V,m)\xi - \zeta, \qquad (2)$$

where $\xi=V_1-V_2$, $\eta=h_1-h_2$, and $\zeta=m_1-m_2$ are infinitesimal perturbations of the zero equilibrium state of Eq. (2), which represents in-phase synchronization. In Eq. (2), $\{V(t),h(t),m(t)\}$ corresponds to the synchronous bursting rhythm. The terms $S_1=-g_s\Gamma(V-\Theta_{\text{syn}})$ and $S_2=g_s(V-E_s)\Gamma_V(V-\Theta_{\text{syn}})$ are due to the synaptic coupling. Note that $S_1\leq 0$ and therefore *stabilizes* the zero equilibrium state of Eq. (2). More precisely, $S_1<0$ after the membrane potential $V(t)$ goes over the synaptic threshold Θ_{syn} as in the case of excitatory coupling [16]. Meanwhile, $S_2\geq 0$ due to $(V-E_s)>0$ and positiveness of the partial $\Gamma_V(V-\Theta_{\text{syn}})$ reaching the high peak at $V=\Theta_{\text{syn}}$ and then rapidly decaying away from the threshold. Consequently, $S_2\xi$ tends to destabilize the origin every time the membrane potential $V(t)$ gets close to Θ_{syn}. In simple terms, the inhibition has a *dual* role in stabilizing and breaking in-phase synchronization as the terms S_1 and S_2 compete with each other to make the synchronous solution stable versus unstable. The overall out-

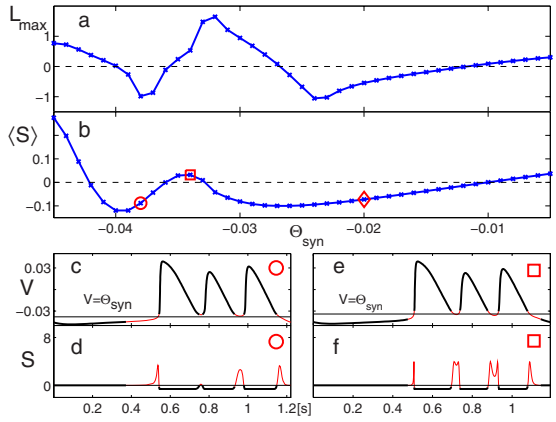

FIG. 4. (Color online) (a) Largest transversal Lyapunov exponent, $L_{\max}$, of synchronous bursting plotted against the synaptic threshold Θ_{syn} at $g_s=0.3$. Note two stability intervals where $L_{\max}<0$. (b) Dependence of averaged $\langle S\rangle=\langle S_1+S_2\rangle$ on Θ_{syn}. Observe the graph of $\langle S\rangle$ closely following that of $L_{\max}$ within the physiologically relevant interval $[-0.025;0.015]$ for Θ_{syn}. It accurately predicts the critical threshold $\Theta_{\text{syn}}=-0.009$ beyond which in-phase synchronization breaks down. Insets (c,d) and (e,f) are similar to Figs. 3(a) and 3(b) and relate to the thresholds Θ_{syn} marked by the circle and the square in (b), corresponding to stable and unstable in-phase synchronization, respectively. When the spikes hit Θ_{syn} transversally [(c) and (d) and Figs. 3(a) and 3(b)], the impact of S_2 is weaker, so that $\langle S\rangle$ remains negative long enough to ensure stable in-phase synchronization. When Θ_{syn} touches spikes from below (e) and (f), the desynchronizing term $\langle S_2\rangle$ lasts longer, thus making $\langle S\rangle$ positive and breaking in-phase synchronization down.

come depends on various quantitative factors including the coupling strength and the level of the synaptic threshold. Whenever the phase point, corresponding to the instantaneous state of one cell, gets close to the threshold Θ_{syn}, the other cell receives a strong short-term desynchronizing kick due to S_2, which causes the divergence between the phase points. Once both rise above the threshold, the inhibition switches into a synchronizing role. Then the phase points receive a weaker though longer lasting synchronizing impact due to S_1, which converges the cells' states, as illustrated in Figs. 3(a) and 3(b). The threshold value Θ_{syn} and the synaptic strength g_s are two crucial factors determining the stability of the zero equilibrium state in variational Eq. (2), and, hence, the stability of in-phase synchronization. Note that the choice of Θ_{syn} affects the balance between the competing terms S_1 and S_2 and may reverse the overall contribution of the coupling from negative to positive and vice versa. That is, raising the threshold closer to the upper part of the spikes lowers the contribution of the stabilizing term S_1 and leads to antiphase bursting in the network (see Figs. 4 and 5).

It is worth noticing that the values of Θ_{syn} from the left interval of stability [see Fig. 4(a)] range from about -0.038 to -0.036. For these values, the threshold Θ_{syn} is placed below the minimum value of spikes and cannot intersect the bursting part of the trajectory and, hence, cannot account for the presence of spikes in the presynaptic cell. As far as the synaptic coupling between the cells is concerned, this location of the synaptic threshold Θ_{syn} implies an interaction that is similar to that between spiking (nonbursting) cells [2].

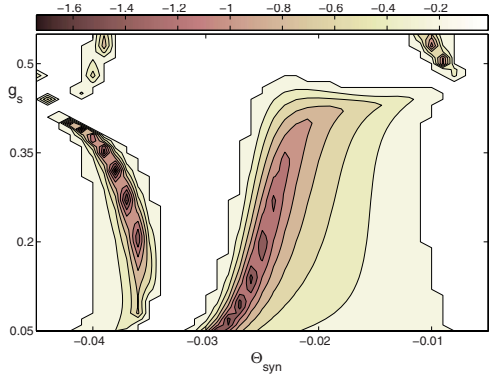

FIG. 5. (Color online) Stability islands for in-phase synchronization in the $(\Theta_{\text{syn}},\ g_s)$-parameter diagram. Level curves of the Lyapunov exponent $L_{\max}$ show two large islands of stable synchrony, where $L_{\max}<0$. Darker shading (top color bar) corresponds to smaller values of $L_{\max}$. Given a fixed threshold Θ_{syn}, increasing the synaptic coupling strength g_s makes synchronization more robust first, but excessively strong inhibition begins desynchronizing the neurons. Note that the vertical axis scale does not extend down to $g_s=0$. The Lyapunov exponent $L_{\max}$ can still be negative below the level $g_s=0.05$; however, its values are close to 0 and sensitive to the choice of the integration method.

Here, the synaptic coupling is always switched on when the systems is on the bursting manifold and switched off when the system is on the quiescent branch of the solution. Stable synchronization observed in this interval is fragile as lowering the threshold closer to the quiescent part switches on the destabilizing term S_2 in a small vicinity of the quiescent part of the synchronous trajectory where the effect of S_2 becomes significant. Therefore, the synchronous solution receives a long lasting desynchronizing impact during the quiescent part and destabilizes. At the same time, the right physiologically relevant interval of Θ_{syn} corresponds to the spike interactions during the active phase of bursting and, therefore, to more robust synchronization. It is important to stress that the evaluation of the averaged synaptic term from the variational equations predicts the synchronization threshold rather precisely and serves as the necessary quantitative condition for stable in-phase synchronization. This calculation is particularly important for the bistable network where coexisting antiphase bursting typically dominates over in-phase synchronization such that it is easy to come to the wrong conclusion that in-phase synchronization is always unstable, relying only on numerical calculations from random initial conditions. Indeed, if one cell is initially in the spiking phase, whereas the other is in quiescence, fast nondelayed reciprocal inhibition between the cells leads only to antiphase bursting. However, if the cells start firing in the spiking phase, then the inhibition, instead of diverging them, will force the cells' states to come together, resulting in stable synchronized bursting. Note that once antiphase bursting is achieved, it remains highly resistant to external voltage perturbations of either cell. On the contrary, a weak common inhibition applied to both cells can break the antiphase regime and make the cells burst together [19] so that the reciprocal inhibition between the cells could synchronize them.

The synchronizing effect of fast nondelayed reciprocal in-

hibition is defined by the intrinsic property of the fast synaptic coupling to act differently on the synchronization trajectory, depending on whether the trajectory crosses or is above the synaptic threshold. This property is linked to the presence of the two competing terms S_1 and S_2 in the variational equations. In this context, it is generic and applicable to other Hodgkin-Huxley-type neurons, exhibiting different types of bursting. In support of this claim, we have examined the synchronization properties of network (1), composed of two coupled (i) Sherman pancreatic β-cell models [13], displaying square-wave bursting; (ii) Purkinje bursting cell models [20]; and (iii) FitzHugh-Rinzel elliptic bursters [14]. In all the three networks, we have observed stable and robust in-phase synchronization, which coexists with antiphase bursting. We have also verified the persistence of robust in-phase synchronization in network (1), after the synaptic FTM function was replaced by the Heaviside function [11] and by a precise dynamical model of fast synapses, wiring the heart beat central patter generator of the leech [15]. In the latter case, the synapses are noninstantaneous yet fast so that the impact of inhibition on synchronization is identical to those of the instantaneous FTM coupling. We have also tested the robustness of in-phase synchronization with respect to mismatches in the synaptic strengths and the intrinsic parameters of the cells. Perfect synchronization is no longer possible in these cases, due to symmetry breaking, resulting in that the spikes within the synchronized burst do not coincide anymore. In all simulated cases this approximative (burst) synchronization has been verified to be robust for a mismatch in the synaptic strengths up to 5–10 %.

In summary, we present the general ability of fast nondelayed reciprocal inhibition to synchronize bursting cells. This synchronizing property is independent from the type of the individual bursting cell and the model of the fast nondelayed inhibition, be it the instantaneous FTM coupling or a dynamical synapse with the synaptic constants comparable with the duration of the presynaptic spike. The exact synergetic features that make stable in-phase synchronization possible are (i) the ability of fast inhibition to switch its impact from desynchronizing to synchronizing when the spikes cross the synaptic threshold and (ii) the presence of spikes in bursts. It is customary in biophysics to use relaxation oscillators as simplified models of bursting cells where the spikes are smoothed over and ignored. However, reciprocally coupled relaxation oscillators with fast nondelayed inhibition are impossible to synchronize [2,11]. In light of this, our result, that the addition of spikes to the individual cell model can reverse the role of fast inhibition from desynchronization to synchronization, is imperative for biophysical modeling of neuronal networks. It stresses the importance of full-scale detailed models of bursting cells versus simplified models such as relaxation oscillators. The two-cell network that we have studied is the fundamental building element of large realistic inhibitory networks. Our preliminary results show that such complex networks with fast inhibitory connections also possess the hidden property to produce the in-phase synchronized rhythm, provided that the individual cells are bursters, not spikers. A consequence is the enhanced multistability of complex neuronal networks, resulting in richer dynamical information capacity and spatiotemporal neuronal integration.

This work was supported by the GSU Brains and Behavior program and the RFFI Grants No. N 08–01–00083 and No. 09–01–00498-a.

[1] T. G. Brown, Proc. R. Soc. London, Ser. B **84**, 308 (1911).

[2] N. Kopell and G. B. Ermentrout, in *Handbook of Dynamical Systems*, edited by B. Fiedler (Elsevier, Amsterdam, 2002), Vol. 2, pp. 3–54.

[3] F. Skinner, N. Kopell, and E. Marder, J. Comput. Neurosci. **1**, 69 (1994); E. Marder and R. L. Calabrese, Physiol. Rev. **76**, 687 (1996); K. L. Briggman and W. B. Kristan, Annu. Rev. Neurosci. **31**, 271 (2008).

[4] X.-J. Wang and J. Rinzel, Neural Comput. **4**, 84 (1992).

[5] J. Rinzel, in *Mathematical Topics in Population Biology, Morphogenesis, and Neurosciences*, Lecture Notes in Biomathematics (Springer, Berlin, 1987), Vol. 71, pp. 267–281; D. Terman, SIAM J. Appl. Math. **51**, 1418 (1991); E. M. Izhikevich, Int. J. Bifurcation Chaos Appl. Sci. Eng. **10**, 1171 (2000); V. N. Belykh, I. V. Belykh, M. Colding-Joergensen, and E. Mosekilde, Eur. Phys. J. E **3**, 205 (2000); A. Shilnikov, R. L. Calabrese, and G. Cymbalyuk, Phys. Rev. E **71**, 056214 (2005); P. Channell, G. Cymbalyuk, and A. Shilnikov, Phys. Rev. Lett. **98**, 134101 (2007); F. Frohlich and M. Bazhenov, Phys. Rev. E **74**, 031922 (2006).

[6] A. Shilnikov and G. Cymbalyuk, Phys. Rev. Lett. **94**, 048101 (2005).

[7] C. Van Vreeswijk, L. F. Abbott, and G. Bard Ermentrout, J. Comput. Neurosci. **1**, 313 (1994).

[8] J. Rubin and D. Terman, in *Handbook of Dynamical Systems*, edited by B. Fiedler (Elsevier, Amsterdam, 2002), Vol. 2, pp. 93–148.

[9] J. Rubin and D. Terman, Neural Comput. **12**, 597 (2000).

[10] D. Golomb and J. Rinzel, Phys. Rev. E **48**, 4810 (1993); D. Terman, N. Kopell, and A. Bose, Physica D **117**, 241 (1998); R. C. Elson, A. I. Selverston, H. D. I. Abarbanel, and M. I. Rabinovich, J. Neurophysiol. **88**, 1166 (2002).

[11] J. Rubin and D. Terman, SIAM J. Appl. Dyn. Syst. **1**, 146 (2002).

[12] D. Somers and N. Kopell, Biol. Cybern. **68**, 393 (1993); N. Kopell and D. Somers, J. Math. Biol. **33**, 261 (1995).

[13] A. Sherman, Bull. Math. Biol. **56**, 811 (1994); B. Lading *et al.*, Prog. Theor. Phys. **139**, 164 (2000).

[14] E. M. Izhikevich, SIAM Rev. **43**, 315 (2001); M. Dhamala, V. K. Jirsa, and M. Ding, Phys. Rev. Lett. **92**, 028101 (2004).

[15] G. S. Cymbalyuk, Q. Gaudry, M. A. Masino, and R. L. Calabrese, J. Neurosci. **22**, 10580 (2002).

[16] I. Belykh, E. de Lange, and M. Hasler, Phys. Rev. Lett. **94**, 188101 (2005).

[17] A. Shilnikov, R. Gordon, and I. Belykh, Chaos **18**, 037120 (2008).

[18] N. Kopell and G. B. Ermentrout, Proc. Natl. Acad. Sci. U.S.A. **101**, 15482 (2004).

[19] I. Belykh and A. Shilnikov, Phys. Rev. Lett. **101**, 078102 (2008).

[20] M. A. Kramer, R. D. Traub, and N. J. Kopell, Phys. Rev. Lett. **101**, 068103 (2008).